International Journal of Biochemistry and Cell Biology 117 (2019) 105626

Contents lists available at ScienceDirect

International Journal of Biochemistry and Cell Biology

journal homepage: www.elsevier.com/locate/biocel

LncRNA625 inhibits STAT1-mediated transactivation potential in esophageal cancer cells

Guo-Wei Huang[a,b,c], Chun-Quan Li[d], Lian-Di Liao[a,b], Ji-Wei Jiao[b,c], Lin Long[b,c], Ji-Yu Ding[b,c], Jin-Cheng Guo[b,c], Li En-Min[b,c,**], Xu Li-Yan[a,b,*]

[a] Institute of Oncologic Pathology, Shantou University Medical College, Shantou, Guangdong, 515041, PR China
[b] The Key Laboratory of Molecular Biology for High Cancer Incidence Coastal Chaoshan Area, Shantou University Medical College, Shantou, Guangdong, 515041, PR China
[c] Department of Biochemistry and Molecular Biology, Shantou University Medical College, Shantou, Guangdong, 515041, PR China
[d] School of Medical Informatics, Daqing Campus, Harbin Medical University, Daqing, 163319, PR China

ARTICLE INFO

Keywords:
LncRNA625
STAT1
IFITM2
TC45
Interaction

ABSTRACT

Although Signal transducer and activator of transcription 1 (STAT1)-mediated transactivation potential is inhibited in cancer cells, the mechanism is poorly understood. In the present study, we implicated long non-coding RNA *lncRNA625* in the inhibition of STAT1 activity. *LncRNA625* knockdown up-regulated STAT1-mediated transcription and resulted in an increase of STAT1-mediated expression of *IFITM2*. Conversely, *lncRNA625* upregulation inhibited STAT1 reporter activity. Mechanistically, *lncRNA625* inhibited STAT1 binding to the promoter of *IFITM2* in both untreated cells and following interferon-gamma (IFN-γ) stimulation. *LncRNA625* interacted with the DNA-binding (DB) domain of STAT1 and promoted STAT1 interaction with T-cell protein tyrosine phosphatase TC45 to dephosphorylate pSTAT1. Taken together, the results show that lncRNA625 inhibits STAT1-mediated transactivation potential by causing formation of STAT1-TC45 complexes, resulting in STAT1 dephosphorylation.

1. Introduction

STAT1, often considered a tumor suppressor, inhibits tumorigenesis and proliferation of tumor cells and promotes tumor cell apoptosis, although in some types of cancer cells, STAT1-mediated tumor progression has been reported, e.g. breast cancer (Hix et al., 2013). Evidence shows that high expression of STAT1 is positively correlated with improved disease-free survival and total survival (Josahkian et al., 2018). However, in malignant cells, STAT1 is subjected to inappropriate activation or even loss of expression. For example, Leibowitz et al. demonstrated that activated STAT1 was present at low to undetectable levels in squamous cell carcinoma of head and neck, and resulted in low expression of the antigen processing protein TAP1/2, thereby enabling cancer cell escape from recognition by cytotoxic T lymphocytes (Leibowitz et al., 2011). Osborn et al. reported that metastatic melanoma cells evaded immune detection by silencing STAT1 (Osborn and Greer, 2015). Recently, Zhang et al. also showed that STAT1 activity was decreased in esophageal cancer cells, and overexpression of STAT1C (its constitutively-active form) inhibited STAT3 activity indispensable for proliferation and survival of tumor cells

Abbreviations: B2M, Beta 2 microglobulin; *Bax*, Bcl-2 associated protein X; *BIRC3*, Baculoviral IAP repeat-containing 3; *CAP1*, Adenylyl cyclase-associated protein 1; *CASP8*, Caspase 8; *CCL2*, C-C motif chemokine 2; *DNMT1*, DNA Methyltransferase 1; *EZH2*, Enhancer of zeste homolog 2; HCP5, HLA Complex P5; *HSPA1A*, Heat Shock Protein Family A (Hsp70) Member 1A; ESCC, Esophageal squamous cell carcinoma; *HSPA1B*, Heat Shock Protein Family A (Hsp70) Member 1B; *ICAM1*, Intercellular adhesion molecule 1; *IFI6*, Interferon alpha inducible protein 6; *IFI44*, Interferon alpha inducible protein 6; *IFIT1*, Interferon induced protein with tetratricopeptide repeats 1; *IFIT3*, Interferon induced protein with tetratricopeptide repeats 3; *IFITM2*, Interferon induced transmembrane protein 2; IFN-γ, interferon γ; *ILR3*, iaa-leucine resistant 3; *KLF2*, Kruppel-like factor 2; *LncRNA625*, long non-coding RNA 625; PRC2, polycomb repressive complex 2; *LMC2*, Laminin subunit gamma-2; *LRG1*, Leucine-rich-alpha-2-glycoprotein 1; *LSD1*, Lysine-specific histone demethylase 1A; *MUC16*, membrane-associated mucin 16; STAT1, Signal transducer and activator of transcription 1; STAT3, Signal transducer and activator of transcription 3; STAT1C, constitutively-active form of STAT1; TC45, 45-kDa T cell protein tyrosine phosphatase; pSTAT1, phosphorylated Signal transducer and activator of transcription 1; *SERPINB4*, Serpin Family B Member 4; TAP1/2, Transporter associated with antigen processing (TAP) protein 1 and 2; *TNFAIP2*, TNF alpha induced protein 2

* Corresponding authors at: Institute of Oncologic Pathology, Shantou University Medical College, No. 22, Xinling Road, Shantou, Guangdong, 515041, China.
** Corresponding author.
E-mail addresses: nmli@stu.edu.cn (L. En-Min), lyxu@stu.edu.cn (X. Li-Yan).

https://doi.org/10.1016/j.biocel.2019.105626
Received 2 June 2019; Received in revised form 26 September 2019; Accepted 30 September 2019
Available online 09 October 2019

(Zhang et al., 2014). Therefore, the above evidence shows that STAT1 activity is inhibited in cancer cells. However, the molecular mechanisms responsible for the inhibition of STAT1 activity are unclear.

Long noncoding RNAs (lncRNAs) participate in cellular processes through various mechanisms (McHugh et al., 2015; Gong and Maquat, 2011; Tripathi et al., 2010). In our previous study, *lncRNA625* was identified as a novel regulator of cell proliferation, invasion and migration in esophageal squamous cell carcinoma (ESCC), and ESCC patients with high *lncRNA625* expression had shorter survival time than those with low expression (Li et al., 2017). In the present study, we characterize the mechanisms of action of *lncRNA625* and show that this lncRNA interacts with STAT1 and directly inhibits the activities of STAT1, thereby playing a key role in the biology of ESCC cells.

2. Results

2.1. LncRNA625 regulates STAT1-mediated gene transcription

In our previous report, we analyzed these genes that were differentially expressed more than ± 1.5-fold between human esophageal squamous carcinoma KYSE150 cell line expressing shRNA-*lncRNA625* and a scrambled shRNA (GSE74707) (Li et al., 2017). In the present study, using R package gplots from the R-project database, we re-analyzed our previous gene profile data (GSE74707) (Li et al., 2017) comparing *lncRNA625*-silenced and control ESCC cells, using a cutoff of fold change = 2. Some differentially expressed genes were found, as shown in Supplementary Fig. S1A. Importantly, upon further GO annotation and functional enrichment analysis, the immune response was significantly enriched, which was shown as the bottom column (Fig. 1A), suggesting that some of these genes were associated with immune or inflammatory processes, e.g. *IFI6, IFIT1, IFI44, IFIT3, IFITM2* and *B2M* (Fig. 1B). And strikingly, in all differentially expressed genes, these genes associated with immune or inflammatory processes accounted for 33.3% of all de-regulated transcripts (Fig. 1B). JASPAR motif analysis for these genes involved in immune response identified numerous potential STAT1 binding motifs at the promoters of these genes (Fig. 1C). To verify the gene profile results, a few candidate genes were subjected to qRT-PCR detection after *lncRNA625* down-regulation. The results showed that the levels of the target genes were altered in response to *lncRNA625* knockdown in KYSE150 cells, including up-regulation of *CCL2, IFIT3* and *IFITM2*, and down-regulation of *HSPA1B, MUC16, HSPA1A, CAP1* and *SERPINB4* (Fig. 1D). In human esophageal squamous carcinoma KYSE180 cells, a decrease of the *SERPINB4* transcript and increases in *CCL2, IFIT3* and *IFITM2* transcripts were further confirmed after *lncRNA625* knockdown (Supplementary Fig. S1B). Subsequently, the above target genes were measured after knockdown of STAT1, with the results showing that the levels of *IFITM2, IFIT3* and *MUC16* were down-regulated in response to STAT1 knockdown (Fig. 1E). These results suggest that *lncRNA625* is involved in the regulation of STAT1-mediated target gene transcription.

2.2. LncRNA625 inhibits STAT1 transactivation potential

We next investigated the functional role of *lncRNA625* involvement in STAT1-regulated gene expression. To this end, we focused on *IFITM2*, as its promoter contained STAT1 binding sites, as predicted by JASPAR (Fig. 2A) and validated by STAT1 ChIP-seq data analysis in the chronic myelogenous leukemia K562 and cervical cancer Hela S cell lines (Fig. 2B), which was downloaded from the Encode database (https://www.encodeproject.org/). STAT1 ChIP-seq data showed that, in the upstream region of *IFITM2* promoter, there were some peaks, suggesting STAT1 binding to the region to regulate the transcription of *IFITM2*. To further confirm STAT1 binding to the promoter of *IFITM2*, STAT1 ChIP was performed and the enriched DNA was amplified by the designed primers targeting the upstream regions of *IFITM2* promoter in Fig. 2A. The results showed that the relative enrichment for STAT1 binding to the promoter of *IFITM2* was significantly higher than that of IgG control, which confirmed that *IFITM2* was the target gene of STAT1 (Fig. 2C). To delineate the role of *lncRNA625* for STAT1 binding to the promoters, STAT1 ChIP-qPCR was performed after *lncRNA625* knockdown. Following *lncRNA625* knockdown, binding of STAT1 to the *IFITM2* promoter was increased (Fig. 2D), indicating that *lncRNA625* inhibited STAT1 binding. To further explore whether the inhibition of *lncRNA625* for STAT1 binding has caused the alteration of STAT1 transactivation potential, luciferase assays were next performed by co-transfection of a STAT1 reporter vector with the *lncRNA625* expression vector. Results showed that *lncRNA625* up-regulation led to the decrease of luciferase activity of STAT1 reporter vector. Therefore, the above data shows that *lncRNA625* inhibits STAT1 transactivation potential (Fig. 2E).

2.3. LncRNA625 inhibits STAT1 transactivation potential induced by IFN-γ

The above data prompted us further to explore how *lncRNA625* regulates the transactivation potential of STAT1. IFN-γ, a well-established STAT1 stimulator, was first studied. KYSE150 cells were treated by IFN-γ as the indicated concentration and the levels of IFITM2 protein were measured using western blot. IFITM2 protein level was significantly enhanced when IFN-γ at final concentration 25 ng/ml was used to treat the cancer cells and there was no obvious alteration for IFIMT2 protein levels responding to higher concentration of IFN-γ treatment. Therefore, IFN-γ at final concentration 25 ng/ml was used in the subsequent assays. Next, we further confirmed that IFN-γ strongly activated STAT1 and upregulated total STAT1 and phosphorylated STAT1 protein expression in ESCC cells. And accordingly, the levels of IFITM2 protein were also enhanced (Fig. 3A and B). Importantly, *lncRNA625* silencing followed by IFN-γ treatment potently increased the phosphorylation of STAT1 and the expression of IFITM2, but not for total STAT1 protein expression (Fig. 3C). At the mRNA level, IFN-γ treatment up-regulated levels of the *IFITM2* transcript (compare black and white columns in Fig. 3D). Upon *lncRNA625* silencing, transcript levels of *IFITM2* strongly increased (compare green and blue columns in Fig. 3D). Further study also showed that IFN-γ treatment promoted an increase of STAT1 binding to *IFITM2* promoter, which was demonstrated by STAT1 ChIP-qPCR. The primers targeting the promoter of *IFITM2* were used for PCR amplification and the results showed that, compared to control, in IFN-γ treatment, there was relative enrichment of STAT1 in the primer I1 and primer I2 targeting regions (Fig. 3E). To exclude the increase of binding of STAT1 to the promoter of *IFITM2* was not derived from the decrease of *lncRNA625* expression in the cells under IFN-γ treatment, we also measured the expression of *lncRNA625* by qRT-PCR. The results showed that IFN-γ treatment did not alter the expression of *lncRNA625* in the cells (Supplementary Fig. S2). Next, to explore the role of *lncRNA625* for the binding of STAT1 to the promoter, STAT1 ChIP-qPCR assays were performed after *lncRNA625* knockdown followed by IFN-γ treatment. ChIP-qPCR assays showed that the binding of STAT1 to the *IFITM2* promoter was enhanced (Fig. 3F). These above data demonstrate that *lncRNA625* inhibits STAT1 transactivation potential induced by IFN-γ.

2.4. LncRNA625 interacts with STAT1 and promotes the interaction STAT1 with TC45

To observe whether *lncRNA625* inhibited STAT1 activity through a direct interaction with STAT1, RIP assays were performed in KYSE150 and KYSE510 cells. Results showed that *lncRNA625* interacted with STAT1 (Fig. 4A). RNA pulldown assays using biotinylated *lncRNA625* further confirmed the interactions between *lncRNA625* and STAT1 (Fig. 4B). To map the regions through which *lncRNA625* interacted with STAT1, we first constructed vectors expressing either full-length or deletion mutants (135 bp, 200 bp, 416 bp) (Fig. 4C, *left*), which were predicted by the minimum free energy (MFE) and partition function to

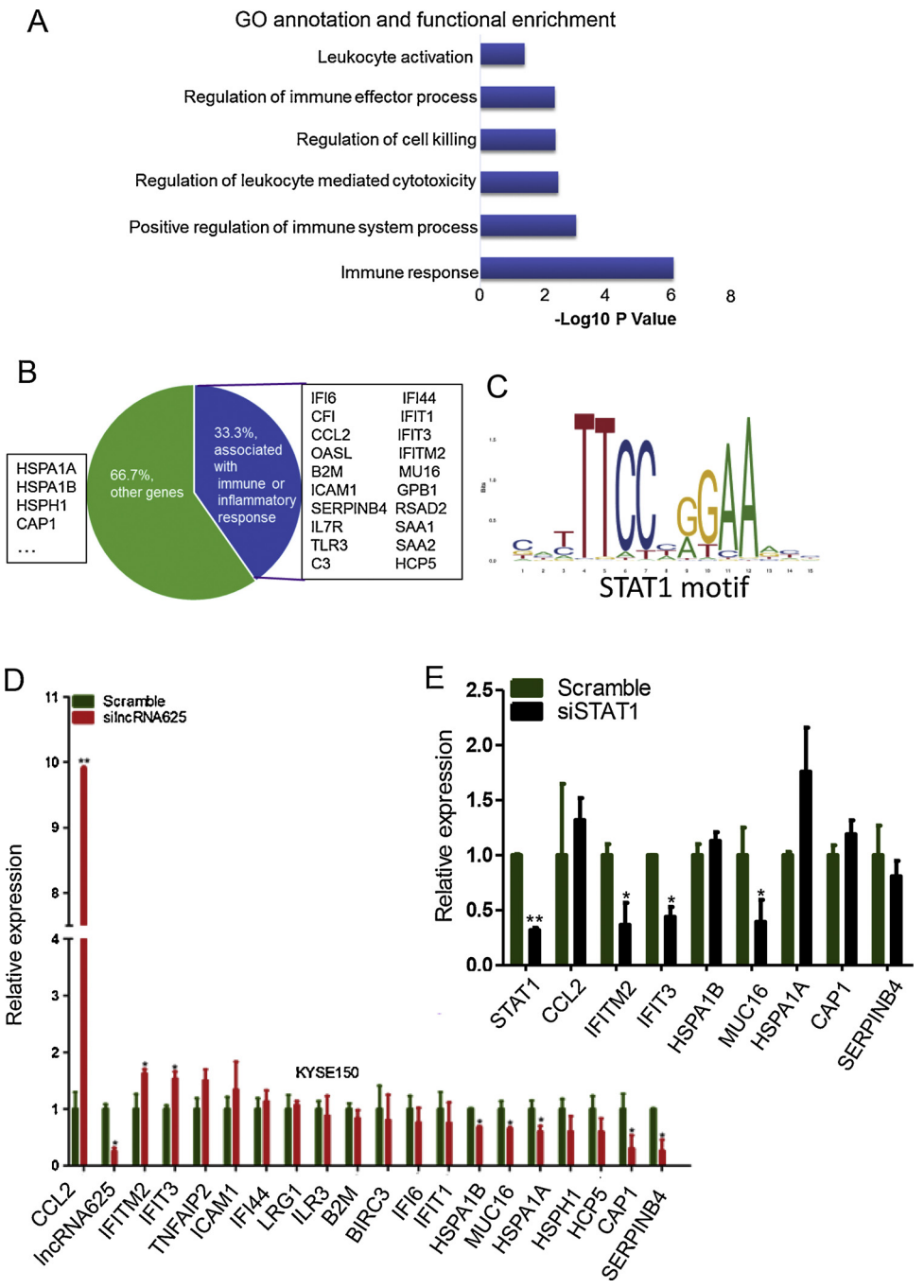

Fig. 1. *LncRNA625* modulates the expression of potential genes induced by STAT1. (A) GO annotation and functional enrichment analysis of genes, from the gene profile, with more than ± 2-fold change. (B) Venn diagram showing genes associated with immunological and inflammatory responses, and other genes. (C) STAT1 binding site motif, in the promoter of potential target genes, predicted by JASPAR. (D) Levels of *lncRNA625*, STAT1 and potential target genes were measured by real-time RT-PCR. KYSE150 cells were plated 24 h prior, and siRNAs against *lncRNA625* and STAT1 were individually transfected. Scramble siRNA was used as the negative control. After 48 h, total RNA was extracted and the levels of *lncRNA625*, STAT1 and the potential target genes were detected by real-time RT-PCR. Values represent mean ± SD. $^{*}P < 0.05$, $^{**}P < 0.01$.

have stem loops (Supplementary Fig. S3). This prediction suggested that these regions of *lncRNA625* might interact with STAT1. Importantly, luciferase assays showed that both full-length and *lncRNA625* deletion mutants inhibited activity of the STAT1 reporter (Fig. 4C, *right*). We next characterized which functional domains of STAT1 were responsible for interacting with *lncRNA625*. Subsequently, a series of STAT1 deletion mutants representing different domains, including a protein interaction domain (Int), coiled-coil domain (CC), DNA-binding domain (DB) and C terminus (C-end), were constructed and co-transfected with the *lncRNA625* vector for RIP assays. Results demonstrated that only the DNA-binding (DB) domain of STAT1 is required to maintain *lncRNA625* binding (Fig. 4D).

In our previous study, we reported that *lncRNA625* was predominantly localized in the nucleus by RNA FISH and cytoplasmic and nuclear isolation assays (Li et al., 2017). In the nucleus, TC45 dephosphorylates STAT1 (Kim and Lee, 2007), suggesting that *lncRNA625* recruits TC45 to inactivate STAT1. Therefore, the interaction of TC45 with pSTAT1 was determined in cells after *lncRNA625* knockdown, followed by IFN-γ treatment. *LncRNA625* knockdown led to a decrease in the interaction of TC45 with pSTAT1 (Fig. 4E). Therefore, our data demonstrate that *lncRNA625* promotes STAT1 interaction with TC45.

3. Discussion

Integrating all the data above, we propose a model in which *lncRNA625* inhibits STAT1-dependent transcription (Fig. 5). In response to IFN-γ, STAT1 translocates into the nucleus, where *lncRNA625* directly binds to the STAT1 DB domain. A second way whereby *lncRNA625* blocks STAT1 is by promoting TC45 interaction with STAT1 to dephosphorylate and inactivate STAT1. Therefore, *lncRNA625* inhibits STAT1 activity by the above dual roles in malignant cells.

Increasing evidence showed that lncRNAs played the critical roles

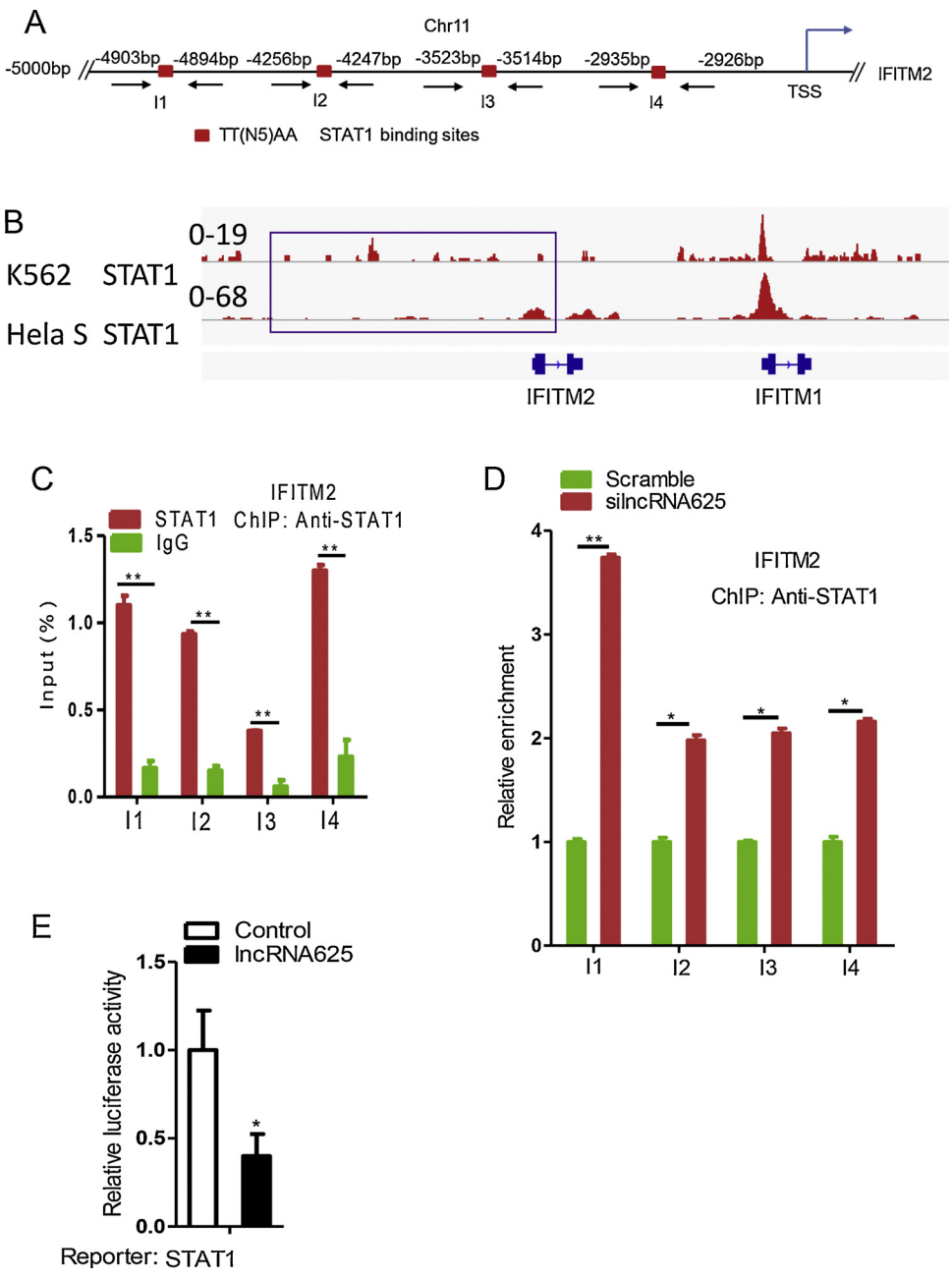

Fig. 2. *LncRNA625* inhibits STAT1 binding to the promoters of potential target genes. (A) Primers for the selected regions of STAT1 binding to *IFITM2* were designed. (B) STAT1 ChIP –seq in K562 and Hela S cell lines from the Encode database (https://www.encodeproject.org/). Representative tracks showing occupancy of the promoter region within the *IFITM2* gene by STAT1. (C) Nuclear extracts of KYSE150 cells (1×10^7 cells) were individually collected in 1 ml, and 10% of each extract was used as input and the remainder used in duplicate for ChIP, using anti-STAT1 and normal rabbit IgG. The coimmunoprecipitated DNA and input DNA were individually extracted and the fold enrichment of STAT1 binding to IFITM2 promoter was determined by qPCR. Rabbit normal IgG was used as the control. The amount of precipitated DNA was calculated as the percent of 100% input according to the method 2x100%. Values represent mean ± SD. $^*P < 0.05$, $^{**}P < 0.01$. (D) After *lncRNA625* knockdown in KYSE150 cells inoculated in 60 mm dishes, ChIP assays were performed as above and the fold enrichment of STAT1 binding to the promoter of IFITM2 was measured according to the method $2^{-[[Ct\ (Treated\ group)\ (STAT1)-Ct(100\%\ Input)]-[Ct\ (Control\ group)\ (STAT1)-Ct(100\%\ Input)]]}$. Scramble siRNA was used as control group. Values represent mean ± SD. $^*P < 0.05$, $^{**}P < 0.01$. (E) The luciferase activity was determined using a dual-luciferase reporter assay system after the *lncRNA625* expression vector with STAT1 reporter plasmid were co-transfected into SHEEC cells. Values represent the mean ± SD of a single experiment done in sextuplicate. $^*P < 0.05$.

for proliferation and metastasis of cancer cells and involved in the regulation of gene expression via various mechanism, including the epigenetic, transcriptional and post-transcriptional regulation for gene expression. lncRNA *HOXA11-AS*, as a scaffold, recruited the chromatin modifying factor PRC2, LSD1 and DNMT1 to regulate the expression of genes and promoted proliferation and invasion of gastric cancer cells (Sun et al., 2016). lncRNA *ANRIL* promoted non-small lung cancer cell proliferation and inhibited apoptosis through the interaction with EZH2 to lead to silence of KLF2 and p21 expression (Nie et al., 2015). LncRNAs implicated in post-transcriptional regulation for gene expression were also reported. LncRNA *SPRY4-IT1*, as a sponge, recruited *miR-101-3p* and thereby up-regulated EZH2 expression, which promoted proliferation and metastasis of bladder cancer cells (Liu et al., 2017). LncRNA *GHET1* increased *c-Myc* mRNA stability and thereby promoted gastric carcinoma cell proliferation (Yang et al., 2014). Numerous evidence showed that, in esophageal squamous carcinoma cells, lncRNAs were involved in proliferation and metastasis and regulated the expression of genes. lncRNA *EZR-AS1* promoted proliferation and invasion through the interaction with SMAD3 and resulting in up-regulation of Ezrin expression (Zhang et al., 2018). LncRNA *CASC9* could promote metastasis of esophageal squamous cell carcinoma. Mechanismly, *CASC9* could form the complex with the transcriptional coactivator CREB-binding protein (CBP) and bind to the *LAMC2* promoter and increase H3K27 acetylation in the promoter, thereby upregulating *LAMC2* expression (Liang et al., 2018). However, in cancer cells, lncRNAs regulating the expression of genes through the interaction with STAT1 are still not reported. In the present study, we found that lncRNA625 promoted the interaction of STAT1 with TC45, which led to dephosphorylation of phosphorylated STAT1 mediated by TC45, thereby inhibiting the transactivation potential of STAT1.

Under IFN-γ stimulation, STAT1 was phosphorylated and subsequently translocated into the nuclei to initiate the transcription of target genes (Olias et al., 2016). In nuclei, TC45, a major nuclear STAT1 protein tyrosine phosphatase (PTPase), dephosphorylated STAT1 (ten Hoeve et al., 2002). Since *lncRNA625* was located in the nuclei (Li et al., 2017), *lncRNA625* knockdown increased the levels of STAT1

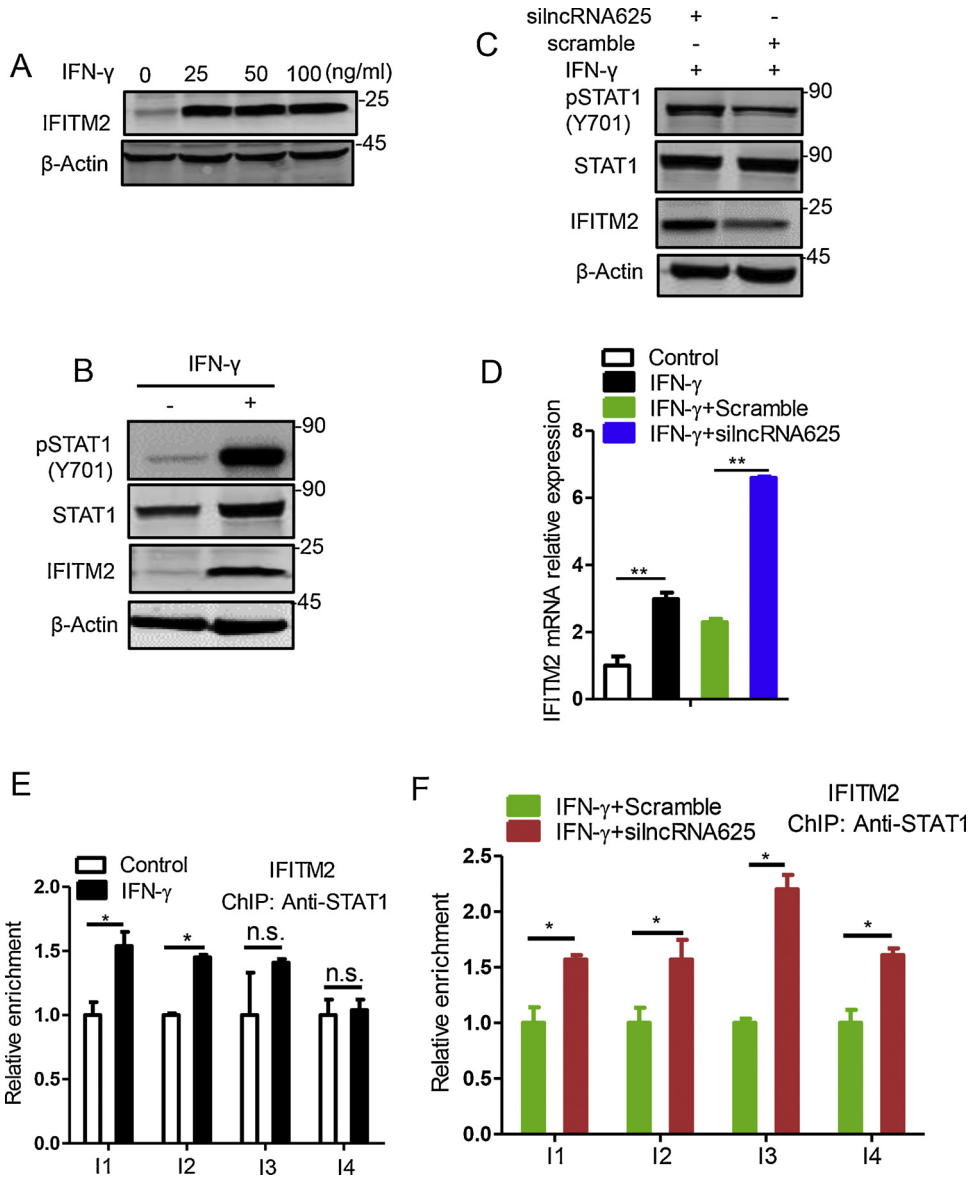

Fig. 3. *LncRNA625* inhibits IFN-γ-mediated STAT1-mediated transcription. (A) In response to IFN-γ at various concentrations, the levels of IFITM2 were characterized using western blot. (B–D) Levels of pSTAT1, STAT1 and IFITM2 were determined using western blot or real-time RT-PCR in KYSE150 cells with or without *lncRNA625* knockdown followed by 25 ng/ml IFN-γ stimulation for 24 h. Values represent mean ± SD. $^{*}P < 0.05$, $^{**}P < 0.01$. KYSE150 cells were cultured in 60 mm dishes and subjected to IFN-γ treatment for 24 h either at 48 h after inoculation (E), or at 24 h post-transfection with si*lncRNA625* or scramble (F), and nuclear extracts were collected and used for ChIP assays of STAT1 as above. The fold enrichment of STAT1 binding to the promoter of IFITM2 was calculated according to the above method. Values represent mean ± SD. $^{*}P < 0.05$, $^{**}P < 0.01$. n.s.: not significant.

phosphorylation (Fig. 3C), suggesting that *lncRNA625* recruited TC45 to prevent STAT1 from being activated. The inhibition of STAT1 activity mediated by *lncRNA625* should prevent apoptosis of cancer cells because STAT1 promoted the transcription of genes associated with pro-apoptosis. E.g. STAT1 promoting the transcription of pro-apoptotic gene Bcl-2 associated protein X (*Bax*) and *CASP8* (Soond et al., 2007; Fulda and Debatin, 2002). In the present study, *IFITM2* was selected as a target gene to delineate the inhibition of *lncRNA625* for STAT1 because *IFITM2* promotes apoptosis of cancer cells (Daniel-Carmi et al., 2009). In fact, it is possible that more potential pro-apoptotic genes associated with STAT1 are regulated by *lncRNA625* in cancer cells. Therefore, it is reasonable that *lncRNA625* recruits TC45 to dephosphorylate STAT1 and thereby inhibits the transcription of pro-apoptotic genes in esophageal cancer cells.

STAT1, as a member of the signal transducers and activators of transcription factor family, interacts with *lncRNA625*. The mechanism for the interaction is still unclear because there is no RNA binding domain in STAT1. However, *lncRNA625* can interact with the STAT1 DB domain. In sum, our results reveal a mechanism by which STAT1 is inhibited in malignant cells, leading to enhanced tumorigenesis. *LncRNA625* can serve as a new therapeutic target for cancer via restoring STAT1 activity through reversal of *lncRNA625*-mediated STAT1 inhibition.

4. Materials and methods

4.1. Cell culture and IFN-γ stimulation

KYSE150, KYSE510 and KYSE180 cell lines derived from human esophageal cancers were cultured in 1640 medium (Hyclone, Logan, UT, USA) supplemented with 10% fetal bovine serum (Hyclone, Logan, UT, USA). HEK293 T cells were derived from human embryonic kidney and kindly provided by Professor Dong Xie (The Institute for Nutritional Sciences, Chinese Academy of Sciences, China). The SHEEC cell line, a normal human ESCC cell line, was established in our laboratory (Shen et al., 2000) and cultured in DMEM/F12 (1:1) medium (Hyclone, Logan, UT, USA) containing 10% newborn bovine serum (Hyclone, Logan, UT, USA). All cell lines were mycoplasma-free and subjected to authentication by STR profiling. In some assays, cells were stimulated with IFN-γ (Sigma Aldrich, St. Louis, Missouri, USA) at the indicated concentration for 24 h.

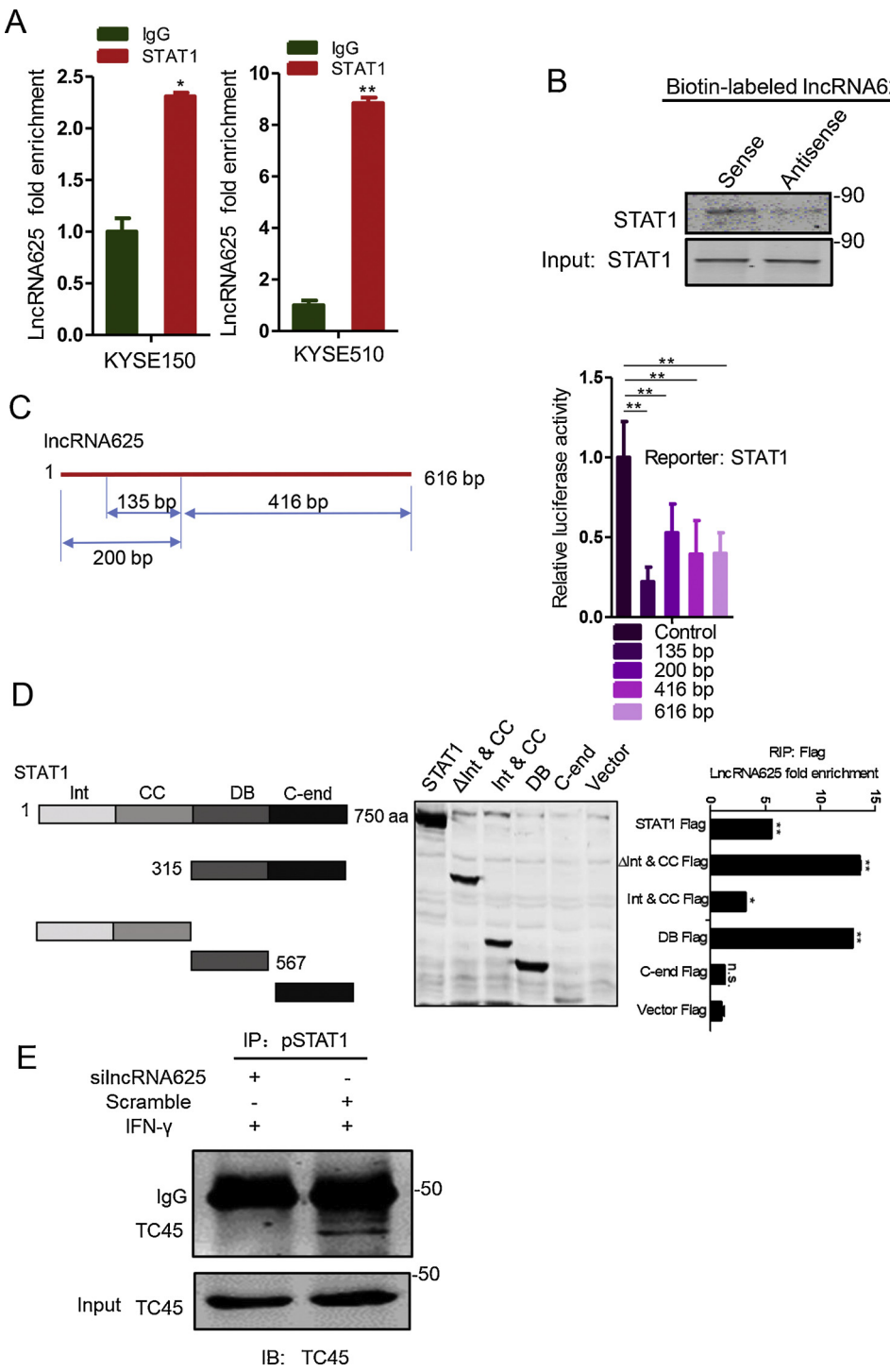

Fig. 4. *LncRNA625* interacts with STAT1 and promotes the interaction of STAT1 with TC45. (A) 1 ml extracts of KYSE150 or KYSE510 cells (1×10^7 cells) were collected and 10% of each extract was used as input, with the rest being used in triplicate for RNA immunoprecipitation using antibodies for rabbit anti-STAT1 or rabbit normal IgG. The co-immunoprecipitated RNA and input RNA was extracted and the fold enrichment of *lncRNA625* was determined by qRT-PCR. Normal rabbit IgG was used as the control. Values represent mean ± SD. $^*P < 0.05$, $^{**}P < 0.01$. (B) Biotinylated *lncRNA625* (sense) or control (antisense) was transfected into KYSE150 cells, then cellular protein extracts were incubated with streptavidin beads and associated proteins were resolved on a gel. Western blotting of the specific association of STAT1 was performed. Input STAT1 was selected as an internal control. (C) Diagram shows full-length *lncRNA625* (616 bp) or *lncRNA625* deletion mutants (135 bp, 200 bp and 416 bp) (*left*). Luciferase activity was determined after co-transfection, into SHEEC cells, of the individual *lncRNA625* or *lncRNA625* deletion mutant expression vector with the STAT1 reporter plasmid (*right*). Values represent mean ± SD of a single experiment done in sextuplicate. $^*P < 0.05$, $^{**}P < 0.01$. (D) Schematic representation of STAT1 protein and different flag fusion proteins (*left*). The flag-STAT1 or different flag fusion protein expression vectors were individually transfected into HEK293 T cells, and flag fusion protein was measured by western blot (*middle*). A flag-RIP assay was employed to detect enrichment of *lncRNA625* in the flag-STAT1 or deletion mutant complex (*right*). Values represent mean ± SD. $^*P < 0.05$, $^{**}P < 0.01$. n.s.: not significant. (E) KYSE150 cells were transfected with si*lncRNA625* or scramble and at 24 h post-transfection, cells were stimulated with IFN-γ for 24 h and nuclear extracts were collected and used for pSTAT1 IP followed by detection of TC45, in the immunoprecipitated complex, by western blot.

4.2. Construction of lncRNA625 deletion mutants and STAT1 mutants

Based on the minimum free energy (MFE) and partition function, MFE and centroid secondary structures of *lncRNA625* (616 bp) and its truncated mutants (416 bp, 200 bp, 135 bp) were predicted online (http://rna.tbi.univie.ac.at/) (Hofacker, 2003). *LncRNA625* and the truncation mutants were individually inserted into the pcDNA3.1 vector, the *lncRNA625* expression vector was previously established in our laboratory (Li et al., 2017), and the vectors expressing *lncRNA625* deletion mutants were constructed by Genewiz (Suzhou, China). Vectors for pcDNA3.1-Flag-STAT1 full-length or deletion mutants composed of various domains, including pcDNA3.1-Flag-C end, pcDNA3.1-Flag-DB, pcDNA3.1- Flag-Int & CC, pcDNA3.1- Flag-ΔInt & CC, were also constructed by Genewiz (Suzhou, China).

4.3. Transfection of siRNAs and plasmids

siRNA or plasmid transfection assays were performed according to previously published procedures (Li et al., 2017). The siRNA sequences were as follows: STAT1: 5′- AAGCAAGCGUAAUCUUCAGdt dt-3′ (sense); 5′ -CUGAAGAUUACGCUUGCUUdtdt-3′ (antisense). Scrambled RNA (negative control): 5′ -UUCUCCGAACGUGUCACGUdt dt-3′ (sense); 5′-ACGUGACACGUUCGGAGAAdtdt-3′ (antisense). siRNAs against *lncRNA625* were synthesized according to our previously

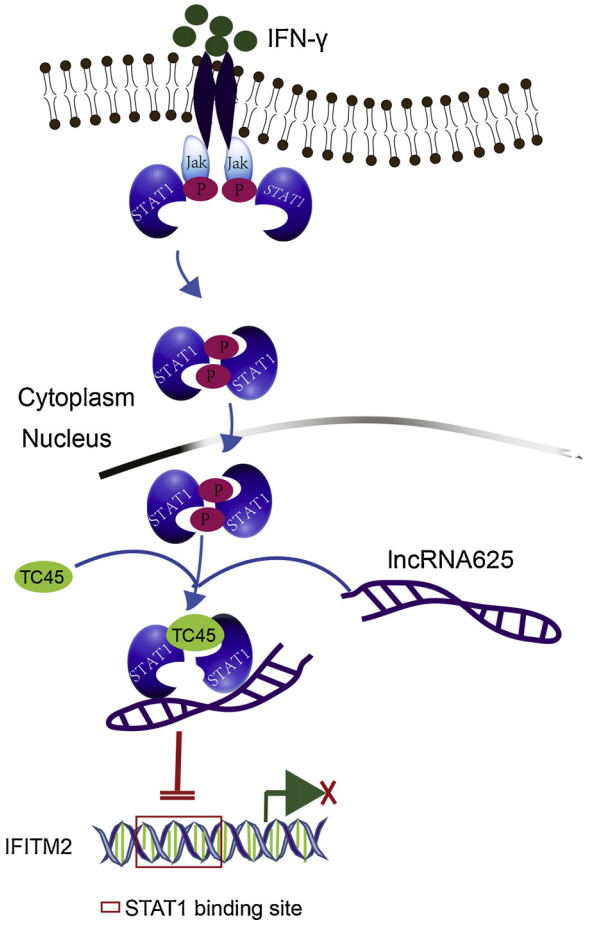

Fig. 5. Schematic diagram indicates that *lncRNA625* inhibits transcription activation activity of STAT1 through inhibiting STAT1 binding to the promoters of target genes and promoting TC45 interaction with STAT1.

published data (Li et al., 2017). All siRNA oligos were synthesized by GenePharma (Suzhou, China).

4.4. Reporter assays

After co-transfection of the vectors of the individual *lncRNA625* with STAT1 (pGL4.45-luc2P/ISRE/hygro-STAT1) reporter vectors, reporter activity of STAT1 was measured using the dual-luciferase reporter assay system (Promega, Madison, WI) according to prior procedures (Zou et al., 2016). In brief, SHEEC cells in 96-well plates were co-transfected using 0.1 μg reporter gene construct and 0.1 μg *lncRNA625* vector together with 4 ng of a Renilla luciferase gene (pRL-TK, Promega, Madison, WI). The pcDNA3.1 vector was used as the control, and transfection of all vectors was performed using Lipofectamine 3000 (Life Technologies, Gaithersburg, MD). After 48 h, firefly luciferase and Renilla luciferase activity were measured using the dual-luciferase reporter assay system on a GloMax® 96 Microplate Luminometer (Promega, Madison, WI, USA).

4.5. Quantitative real-time PCR (qRT-PCR) and western blot

qRT-PCR and western blot were performed according to prior procedures (Huang et al., 2015). In brief, total RNA was extracted with Trizol and the concentration and the purity were determined by OD260/280 using a Nanodrop (Agilent Technologies, Palo Alto, CA, USA). After contaminating genomic DNA was removed by DNase (RR047A, Takara, Dalian, China), 1 μg RNA was reverse-transcribed into cDNA according to the manufacturer's instructions (RR047A, Takara, Dalian, China). qRT-PCR was performed according to the manufacturer's instructions (RR081A, Takara, Dalian, China) using a 7500 Real-Time PCR System (Applied Biosystems, Foster City, CA, USA). The primers for qRT-PCR are shown in Supplementary Table S1. The primer for *lncRNA625* was shown in our previously published data (Li et al., 2017). RNA expression was normalized to the negative control group using $2^{-\Delta Ct\Delta Ct}$ method. Primary antibodies were rabbit anti-pSTAT1, rabbit anti-TC45 (Cell Signal Technology Inc., Danvers, MA), rabbit anti-FLAG (Sigma Aldrich, St. Louis, Missouri, USA) and rabbit anti-STAT1, mouse anti-IFITM2, mouse anti-EP300 and β-actin (Santa Cruz Biotechnology, Santa Cruz, CA, USA) were used for western blotting. IRDye® 800CW goat anti-mouse IgG (H + L) and IRDye® 800CW goat anti-rabbit IgG (H + L) (LI − COR Biosciences, Lincoln, Nebraska, USA) were used as secondary antibodies. A Li-COR Odyssey infrared imager was used for the visualization of protein bands in the western blot (LI-COR Biosciences, Lincoln, Nebraska, USA). In some cases, the vectors for STAT1 full-length or the deleted mutants were individually transfected into HEK293 T cells and total protein was extracted and subjected to 15% gel electrophoresis, followed by transfer to nitrocellulose at 60 V for 60 min. STAT1 full-length or the deleted mutants were determined by using rabbit anti-FLAG and IRDye® 800CW goat anti-rabbit IgG (H + L) (LI-COR Biosciences, Lincoln, Nebraska, USA).

4.6. RNA immunoprecipitation and Co-immunoprecipitation (Co-IP)

RNA immunoprecipitation was performed as previously described (Huang et al., 2017a, b). Briefly, KYSE150 or KYSE510 cell extracts were incubated with rabbit anti-STAT1 (Santa Cruz Biotechnology, Santa Cruz, CA, USA) and 10% of each cell extract was used as input. The STAT1 complex was pulled down using protein G coupled to magnetic beads (Life Technologies, Gaithersburg, MD). Normal rabbit IgG was used as the negative control (Santa Cruz Biotechnology, Santa Cruz, CA, USA). In some cases, the co-transfected extracts of pcDNA3.1-*lncRNA625* with pcDNA3.1-Flag-STAT1 or the deletion mutants of STAT1 in HEK293 T cells was individually incubated with rabbit anti-Flag (Sigma Aldrich, St. Louis, Missouri, USA) and cells transfected with the pcDNA3.1 vector were used as negative controls. RNA was extracted from the precipitated complex using 1 ml Trizol (Life Technologies, Gaithersburg, MD) and *lncRNA625* was measured with qRT-PCR. In Co-IP assays, siRNA against *lncRNA625* or scramble was transfected into KYSE150 cells and after 24 h, cells were treated with IFN-γ for 24 h and co-IP was performed using rabbit anti-pSTAT1 (Cell Signal Technology Inc., Danvers, MA), followed by detection of TC45 by western blot.

4.7. Chromatin immunoprecipitation (ChIP)

ChIP assays were performed as previously described (Nelson et al., 2006). KYSE150 cells (1×10^7 cells) were fixed with 1.42% formaldehyde final concentration for 15 min, and then fixations were quenched by adding glycine to 125 mM final concentration for 5 min. Then, cells were scraped and collected by centrifugation at 2000 *g* for 5 min at 4 °C. Cell pellets were resuspended in lysis buffer (150 mM NaCl, 50 mM Tris-HCl (pH 7.5), 5 mM EDTA, NP-40 (0.5% vol/vol), Triton X-100 (1.0% vol/vol)) containing protease inhibitors and phosphatase inhibitors (Sigma Aldrich, St. Louis, Missouri, USA), and supernatant was removed by centrifugation at 12,000 *g* for 1 min at 4 °C after pipetting up and down several times. Nuclear lysates were resuspended in lysis buffer and then sonicated to shear the chromatin to 0.2 ~ 1 kb in size. 10% of extracts were used as input and the remainder were incubated with rabbit anti-STAT1 or normal rabbit IgG (Santa Cruz Biotechnology, Santa Cruz, CA, USA) overnight at 4 °C. The next day, protein–DNA complexes were pulled down using protein G magnetic beads (Life Technologies, Gaithersburg, MD), and the precipitates were resuspended in a 10% (wt/vol) Chelex 100 (Life Technologies,

Gaithersburg, MD) slurry and boiled for 10 min. The total DNA in the 10% input was precipitated with 10 µl 5 M NaCl and 3 volumes of ethanol for 2 h at −20 °C and the dried pellet was then dissolved in 10% (wt/vol) Chelex 100 suspension and boiled for 10 min. After boiling, proteinase K was added to each sample and shaken at 55 °C on a thermal mixer (HYK Gene Sciences, Shenzhen, China) at 1000 rpm/min for 30 min) and then boiled again for 10 min. The supernatant was collected by centrifugation at 12,000 *g* for 1 min at 4 °C, and 120 µl ultrapure water (MilliQ) was added to the beads. After vortex for 10 s, 120 µl of supernatant was collected and pooled with the previous supernatant. The isolated DNA was used for qPCR. The primer sequence for qPCR is in Supplementary Table S1.

4.8. RNA pull-down

Biotin-*lncRNA625* full-length sense or antisense probes were synthesized according to a prior method (Li et al., 2017) with some modifications. In short, a T7 promoter sequence was added to the forward primer for sense probe synthesis, and the reverse primer for the antisense probe. As for probe synthesis, pcDNA3.1-*lncRNA625* was amplified by PCR and the PCR product was used as the in vitro transcription template. Primers for sense probe synthesis were as follows: 5′-GATC ACTAATACGACTCACTATAGGGACATCTAGGAAGTGAGAAGCGTC TC-3′ (forward); 5′-GGCTAATAAACAGGGTCTTCAG GT-3′ (reverse); primers for antisense probe synthesis were 5′-ACATCTAGGAA GTGAGAAGCGTCTC-3′ (forward), 5′-GATCACTAATACGACTCACTATA GGGAAAAACACCAGAGAGGGCATTCGGA-3′ (reverse). The synthesized probes were purified by an RNA clean kit (Bioteke, Beijing, China). Biotin-*lncRNA625* sense or antisense probes were subsequently transfected into KYSE150 cells inoculated in 60 mm dishes 24 h prior according to previously published procedures (Zhang et al., 2018; Huang et al., 2017a, b), and after 48 h, total protein was extracted and STAT1 was measured by western blot.

4.9. Bioinformatics analysis

According to our previous gene profile data (GSE74707) for comparison of KYSE150 cells with shRNA-*lncRNA625* or shRNA-scramble (Li et al., 2017), R package gplots from the R-project database (https://CRAN.R-project.org/package=gplots) (Warnes et al., 2016) were used to do the heatmap for target genes with more than ± 2-fold change. GO annotation and functional enrichment analysis for these target genes were performed according to the DAVID database on line (https://david.ncifcrf.gov/) (Huang et al., 2009). The sequences of the promoters of these target genes associated with the immune or inflammatory response were analyzed by the online JASPAR database (http://jaspar.binf.ku.dk/) (Stormo, 2013; Wasserman and Sandelin, 2004). STAT1 ChIP –seq data in K562 and Hela S cell lines was download from the Encode database (https://www.encodeproject.org/) and the file with format (.bw) was opened with IGV software and the peaks for STAT1 binding to the IFITM2 promoter were shown.

4.10. Statistical analysis

SPSS 19.0 for Windows (IBM, Chicago, IL, USA) was used for statistical analyses. The data between groups was compared by using Student's *t*-test and a two-tailed *p*-value less than 0.05 was considered statistically significant.

Author contributions

LEM and XLY: contributed to the concept and design of the study. HGW, LLD, JJW and LL: performed the experiments. LCQ, DJY and GJC: contributed to statistical and computational analysis. HGW: contributed to the writing of the manuscript. XLY: contributed to the review and revision of the manuscript.

Declaration of Competing Interest

No potential conflicts of interest were disclosed.

Acknowledgements

This work was supported by grants from the National Natural Science Foundation of China (No. 81772532 and No. 81472613), the Natural Science Foundation of China-Guangdong Joint Fund (No. U1601229), the National Cohort of Esophageal Cancer of China (2016YFC0901400) and Guangdong Natural Science Foundation (2018A0303130177).

Appendix A. Supplementary data

Supplementary material related to this article can be found, in the online version, at doi:https://doi.org/10.1016/j.biocel.2019.105626.

References

Daniel-Carmi, V., Makovitzki-Avraham, E., Reuven, E.M., Goldstein, I., Zilkha, N., Rotter, V., Tzehoval, E., Eisenbach, L., 2009. The human 1-8D gene (IFITM2) is a novel p53 independent pro-apoptotic gene. Int. J. Cancer 125, 2810–2819.
Fulda, S., Debatin, K.M., 2002. IFNgamma sensitizes for apoptosis by upregulating caspase-8 expression through the Stat1 pathway. Oncogene 21, 2295–2308.
Gong, C., Maquat, L.E., 2011. LncRNAs transactivate STAU1-mediated mRNA decay by duplexing with 3'UTRs via Alu elements. Nature 470, 284–288.
Hix, L.M., Karavitis, J., Khan, M.W., Shi, Y.H., Khazaie, K., Zhang, M., 2013. Tumor STAT1 transcription factor activity enhances breast tumor growth and immune suppression mediated by myeloid-derived suppressor cells. J. Biol. Chem. 288, 11676–11688.
Hofacker, I.L., 2003. Vienna RNA secondary structure server. Nucleic Acids Res. 13, 3429–3431.
Huang, G.W., Liao, L.D., Li, E.M., Xu, L.Y., 2015. siRNA induces gelsolin gene transcription activation in human esophageal cancer cell. Sci. Rep. 5, 7901.
Huang, G.W., Zhang, Y.L., Liao, L.D., Li, E.M., Xu, L.Y., 2017a. Natural antisense transcript TPM1-AS regulates the alternative splicing of tropomyosin I through an interaction with RNA-binding motif protein 4. Int. J. Biochem. Cell Biol. 90, 59–67.
Huang, R., Zhang, Y., Han, B., Bai, Y., Zhou, R., Gan, G., Chao, J., Hu, G., Yao, H., 2017b. Circular RNA HIPK2 regulates astrocyte activation via cooperation of autophagy and ER stress by targeting MIR124-2HG. Autophagy 13, 1722–1741.
Huang, da.W., Sherman, B.T., Lempicki, R.A., 2009. Systematic and integrative analysis of large gene lists using DAVID bioinformatics resources. Nat. Protoc. 1, 44–57.
Josahkian, J.A., Saggioro, F.P., Vidotto, T., Ventura, H.T., Candido Dos Reis, F.J., de Sousa, C.B., Tiezzi, D.G., de Andrade, J.M., Koti, M., Squire, J.A., 2018. Increased STAT1 expression in high grade gerous ovarian cancer is associated with a better outcome. Int. J. Gynecol. Cancer 28, 459–465.
Kim, H.S., Lee, M.S., 2007. STAT1 as a key modulator of cell death. Cell. Signal. 19, 454–465.
Leibowitz, M.S., Andrade Filho, P.A., Ferrone, S., Ferris, R.L., 2011. Deficiency of activated STAT1 in head and neck cancer cells mediates TAP1-dependent escape from cytotoxic T lymphocytes. Cancer Immunol. Immunother. 60, 525–535.
Li, C.Q., Huang, G.W., Wu, Z.Y., Xu, Y.J., Li, X.C., Xue, Y.J., Zhu, Y., Zhao, J.M., Li, M., Zhang, J., Wu, J.Y., Lei, F., Wang, Q.Y., Li, S., Zheng, C.P., Ai, B., Tang, Z.D., Feng, C.C., Liao, L.D., Wang, S.H., Shen, J.H., Liu, Y.J., Bai, X.F., He, J.Z., Cao, H.H., Wu, B.L., Wang, M.R., Lin, D.C., Koeffler, H.P., Wang, L.D., Li, X., Li, E.M., Xu, L.Y., 2017. Integrative analyses of transcriptome sequencing identify novel functional lncRNAs in esophageal squamous cell carcinoma. Oncogenesis 2, e297.
Liang, Y., Chen, X., Wu, Y., Li, J., Zhang, S., Wang, K., Guan, X., Yang, K., Bai, Y., 2018. LncRNA CASC9 promotes esophageal squamous cell carcinoma metastasis through upregulating LAMC2 expression by interacting with the CREB-binding protein. Cell Death Differ. 25, 1980–1995.
Liu, D., Li, Y., Luo, G., Xiao, X., Tao, D., Wu, X., Wang, M., Huang, C., Wang, L., Zeng, F., Jiang, G., 2017. LncRNA SPRY4-IT1 sponges miR-101-3p to promote proliferation and metastasis of bladder cancer cells through up-regulating EZH2. Cancer Lett. 388, 281–291.
McHugh, C.A., Chen, C.K., Chow, A., Surka, C.F., Tran, C., McDonel, P., Pandya-Jones, A., Blanco, M., Burghard, C., Moradian, A., Sweredoski, M.J., Shishkin, A.A., Su, J., Lander, E.S., Hess, S., Plath, K., Guttman, M., 2015. The Xist lncRNA interacts directly with SHARP to silence transcription through HDAC3. Nature 521, 232–236.
Nelson, J.D., Denisenko, O., Bomsztyk, K., 2006. Protocol for the fast chromatin immunoprecipitation (ChIP) method. Nat. Protoc. 1, 179–185.
Nie, F.Q., Sun, M., Yang, J.S., Xie, M., Xu, T.P., Xia, R., Liu, Y.W., Liu, X.H., Zhang, E.B., Lu, K.H., Shu, Y.Q., 2015. Long noncoding RNA ANRIL promotes non-small cell lung cancer cell proliferation and inhibits apoptosis by silencing KLF2 and P21 expression. Mol. Cancer Ther. 14, 268–277.
Olias, P., Etheridge, R.D., Zhang, Y., Holtzman, M.J., Sibley, L.D., 2016. Toxoplasma effector recruits the Mi-2/NuRD complex to repress STAT1 transcription and block IFN-γ-dependent gene expression. Cell Host Microbe 20, 72–82.
Osborn, J.L., Greer, S.F., 2015. Metastatic melanoma cells evade immune detection by

silencing STAT1. Int. J. Mol. Sci. 16, 4343–4361.
Shen, Z., Cen, S., Shen, J., Cai, W., Xu, J., Teng, Z., Hu, Z., Zeng, Y., 2000. Study of immortalization and malignant transformation of human embryonic esophageal epithelial cells induced by HPV18 E6E7. J. Cancer Res. Clin. Oncol. 126, 589–594.
Soond, S.M., Carroll, C., Townsend, P.A., Sayan, E., Melino, G., Behrmann, I., Knight, R.A., Latchman, D.S., Stephanou, A., 2007. STAT1 regulates p73-mediated Bax gene expression. FEBS Lett. 581, 1217–1226.
Stormo, G.D., 2013. Modeling the specificity of protein-DNA interactions. Quant. Biol. 2, 115–130.
Sun, M., Nie, F., Wang, Y., Zhang, Z., Hou, J., He, D., Xie, M., Xu, L., De, W., Wang, Z., Wang, J., 2016. LncRNA HOXA11-AS promotes proliferation and invasion of gastric Cancer by scaffolding the chromatin modification factors PRC2, LSD1, and DNMT1. Cancer Res. 76, 6299–6310.
Tripathi, V., Ellis, J.D., Shen, Z., Song, D.Y., Pan, Q., Watt, A.T., Freier, S.M., Bennett, C.F., Sharma, A., Bubulya, P.A., Blencowe, B.J., Prasanth, S.G., Prasanth, K.V., 2010. The nuclear-retained non-coding RNA MALAT1 regulates alternative splicing by modulating SR splicing factor phosphorylation. Mol. Cell 39, 925–938.
Warnes, G.R., Bolker, B., Bonebakker, L., Gentleman, R., Huber, W., Liaw, A., Thomas, L., Maechler, M., Magnusson, A., Moeller, S., Schwartz, M., Venables, B., 2016. Gplots: Various R Programming Tools for Plotting Data (comprehensive R Archive Network). R package version 3.0. 1. https://CRAN.R-project.org/package=gplots).
Wasserman, W.W., Sandelin, A., 2004. Applied bioinformatics for the identification of regulatory elements. Nat. Rev. Genet. 4, 276–287.
ten Hoeve, J., de Jesus Ibarra-Sanchez, M., Fu, Y., Zhu, W., Tremblay, M., David, M., Shuai, K., 2002. Identification of a nuclear Stat1 protein tyrosine phosphatase. Mol. Cell. Biol. 22, 5662–5668.
Yang, F., Xue, X., Zheng, L., Bi, J., Zhou, Y., Zhi, K., Gu, Y., Fang, G., 2014. Long non-coding RNA GHET1 promotes gastric carcinoma cell proliferation by increasing c-Myc mRNA stability. FEBS J. 281, 802–813.
Zhang, X.D., Huang, G.W., Xie, Y.H., He, J.Z., Guo, J.C., Xu, X.E., Liao, L.D., Xie, Y.M., Song, Y.M., Li, E.M., Xu, L.Y., 2018. The interaction of lncRNA EZR-AS1 with SMYD3 maintains overexpression of EZR in ESCC cells. Nucleic Acids Res. 46, 1793–1809.
Zhang, Y., Molavi, O., Su, M., Lai, R., 2014. The clinical and biological significance of STAT1 in esophageal squamous cell carcinoma. BMC Cancer 14, 791.
Zou, H.Y., Lv, G.Q., Dai, L.H., Zhan, X.H., Jiao, J.W., Liao, L.D., Zhou, T.M., Li, C.Q., Wu, B.L., Xu, L.Y., Li, E.M., 2016. A truncated splice variant of human lysyl oxidase-like 2 promotes migration and invasion in esophageal squamous cell carcinoma. Int. J. Biochem. Cell Biol. 75, 85–98.